

RADAR IMAGING USING A WIDEBAND ADAPTIVE ARRAY

Mark Curry, Yasuo Kuga
University of Washington, Seattle, WA, USA

Introduction

The focus of this paper is to investigate the application of wideband adaptive array processing techniques to the problem of radar imaging. In particular we are interested in joint range-angle estimation with angular resolution improvement for small, relative to λ , antennas. The simulations and experimental results indicate that this approach is viable in a practical sense, and yields significant angular resolution improvement over conventional methods.

The approach uses conventional Fourier techniques for downrange information and uses adaptive beamforming for the azimuth dimension. The basic approach is to transmit a wideband set of continuous wave signals, then apply spatial resampling to the received data to correct for the fixed element spacing, then Fourier transform this data to extract range information. We then have a spectral estimation problem at each range cell. By using data associated with each range bin, the angular spectrum is computed using a minimum variance spectral estimate. In general, adaptive array theory is based on the narrow band requirement that the array aperture size is much less than the inverse relative bandwidth. This implies that plane waves are parameterized primarily by their angle of arrival. For this work the narrowband assumption is not valid since we will be using bandwidths of at least 20% of the carrier frequency. Spatial resampling can estimate the array data that would occur if the antenna spacing were varied physically as a function of frequency. See [2] for a discussion of spatial resampling applied to underwater acoustics. Another problem that must be addressed is that parametric spectral estimation methods require a covariance matrix to be estimated from multiple, uncorrelated snapshots of the array output. We introduce a method that amounts to an induced Doppler shift that can be used to generate the required data necessary for angular spectral estimates. The final result is a range-angle plot of backscattered energy.

Signal Model and Formulation

Consider the case of a superposition of plane waves incident upon a receiving array. These plane waves are the backscattered energy from objects in the field of view of

the transmitter. Assume objects are in the far field so the plane wave assumption is valid. The incident plane waves can be parameterized by their angle of arrival as shown in Figure 1.

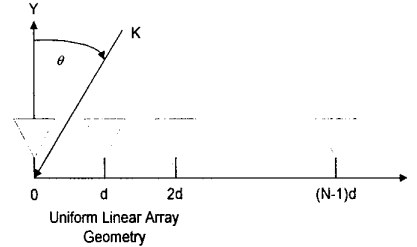


Figure 1. Uniform linear array geometry.

A narrowband incident field with wavenumber vector \vec{k} is present. $|\vec{k}| = k = 2\pi f / c_0$, where c_0 is the free space velocity. In the X-Y plane $\vec{k} = k(\sin \theta, \cos \theta)^T$, with θ measured clockwise from the Y-axis. The sensor positions are given by $\vec{r} = (x_n \ y_n)^T$. The output of each sensor is then given by

$$V(\vec{k}, \vec{r}) = Ae^{-j\vec{k}^T \vec{r}} \quad (1)$$

Applying this to the uniform linear array geometry above yields the baseband output at each sensor as

$$V(n) = Ae^{-jkn d \sin \theta}, n \in 0 : N-1 \quad (2)$$

with d the inter-element distance.

Given that range information requires signal bandwidth, consider a point target at a distance r_0 from the origin. A CW transmitter radiates a field that is scattered by the target back to the receiver. The target is modeled as a delta function with backscattering amplitude, $A(r_0) = A = 1$, at the receiver.

$$B(r) = A(r_0)\delta(r - r_0) \quad (3)$$

The transmitter generates a CW signal at frequency f_m , with round trip travel time given by $\tau_0 = \frac{2r_0}{c_0}$. For

frequency f_m the received signal is:

$$V_o = A e^{-j2\pi f_m (2r_o/c_o)} = A e^{-j2\pi m \Delta f (2r_o/c_o)}, \quad (4)$$

where $\Delta f = \frac{f_{BW}}{M}$ and f_{BW} is the total bandwidth used and M is the number of steps. This equation is the discrete (spatial) frequency Fourier transform of the target position r_o . Note that $\frac{f_{BW}}{c_o}$ has units of cycles per unit distance, or cycles per meter for example. Therefore a point target at position r_o is transformed to M samples of a complex exponential of 'frequency', $\frac{2\Delta f}{c_o} r_o$ or $\frac{2f_{BW}}{Mc_o} r_o$. To convert this signal to the spatial domain, apply the inverse Fourier transform, which yields

$$I(n) = A \sum_{m=0}^{M-1} e^{-j2\pi m (2f_{BW}r_o/Mc_o)} e^{j2\pi m (n/M)}. \quad (5)$$

This equation describes a *SINC* function with peak at $n = \text{round}(\frac{2f_{BW}}{c_o} r)$, where $\text{round}()$ signifies rounding to the nearest integer and r is an arbitrary distance. The *SINC* function provides interpolation for range values that are non-integer values of $\frac{2f_{BW}}{c_o} r$. Increasing the

bandwidth, f_{BW} , will increase the resolution but reduces the maximum usable range due to aliasing. This method of ranging is called FM-CW ranging and is well known for imaging stationary scenes. The free space medium is linear so superposition holds, allowing the extension of one target to multiple targets or in our case scatterers distributed in range (and angle). As will be shown in the next section increasing bandwidth, f_{BW} , also affects the spatial spectrum.

We then combine the FM-CW technique with the angle of arrival results to describe the antenna outputs for the M , CW linear stepped frequencies, with angles of arrival from $-\pi/2$ to $\pi/2$, incident upon N antenna elements. Combining Eq(2) and Eq(4), and letting $A=1$, the baseband antenna output for frequency m and element n , for one emitter at range r_o and angle θ is

$$V_o(n, m) = e^{-j2\pi m \Delta f \frac{2r_o}{c_o}} e^{-j2\pi \frac{f_o}{c_o} n d \sin \theta} e^{-j2\pi (\frac{m}{M} - \frac{1}{2}) \frac{f_{BW}}{c_o} n d \sin \theta}. \quad (5)$$

Transmit frequency, $f_m = f_o + (m - \frac{M}{2})\Delta f$ and f_o is the center frequency of the antenna. The first exponential term describes the phase information for range, and the second and third terms describe the inter-element phase due to the incidence angle. The second term describes the linear phase shift across the array for incidence angle θ , which is independent of frequency. However the third term shows an additional phase across the array which is dependent on frequency $m\Delta f$. The affect of the last term is to cause the angle of arrival to appear to change as the incident field wavelength changes. The angle of arrival sweeps linearly from

$$\frac{2\pi f_o}{c_o} (1 - \frac{f_{BW}}{2f_o}) d \sin \theta \text{ radians}$$

to

$$\frac{2\pi f_o}{c_o} (1 + \frac{f_{BW}}{2f_o}) d \sin \theta \text{ radians}. \quad (6)$$

The angular sweep is proportional to the true angle. For large angles of arrival the angular broadening is greatest. Targets are smeared in range by the third term also. Conventional delay and sum beamforming correctly accounts for both of these affects, but for small antennas the angular resolution will be poor. The set of received signal samples from M frequencies, at N outputs of the antenna array is formed into a matrix for processing.

Spatial Resampling

The array outputs must be properly focussed so that the angle of arrival of a single plane wave for any given frequency m will be constant. This is accomplished by resampling the array outputs to correct for the constant element spacing d . See [4] for discussion of spatial resampling techniques applied to wideband angle of arrival estimation for uncorrelated signals. For joint range-angle estimation we have the additional requirement that the antenna phase center for each resampled array output must remain fixed at the center of the array. The spatial resampling concept is motivated by treating the outputs of the N element linear array as the result of spatially sampling a continuous linear array. The resampling is accomplished by approximating a continuous array by interpolation of the given data and then extracting the required samples at the new sampling interval required for each temporal frequency m . Interpolation is accomplished by inserting $K - 1$ zeros between samples, where K is the interpolation factor, to produce a vector of length KN . A linear phase, low pass filter is applied to the data. This filter has a cutoff frequency of $\frac{\theta}{K}$, where

θ is the maximum normalized spatial angle, typically $\pm \pi/2$. A fast implementation utilizes the polyphase filtering architecture [3]. The resampling process will create a set of data that contains samples at varying distances from the antenna phase center. To prevent the algorithm from trying to sample beyond the ends of the array we introduce a scale factor $\beta = \frac{f_{\min}}{f_o}$, which has the affect of making the interpolated array spacing d appear fractionally smaller than the original by β . Consequently the steering vectors used later for angular spectrum estimation will be corrected by β also. Combining these ideas with the bandwidth relation in (6) it is easily shown that the resampled data for element n , and frequency m , from the interpolated array is given by

$$Y(n, m) = X_{interp} \left(\text{round} \left(\left(\frac{KN}{2} \right) + \frac{K \left(n - \frac{N}{2} \right)}{1 + \frac{BW}{f_o} \left(\frac{m - \frac{M}{2}}{M} \right) \frac{f_{\min}}{f_o}} \right) \right) \quad (7)$$

where $X_{interp}(\ast)$ is the interpolated array of length KN . \mathbf{Y} is a matrix of size M by N . The offsets into the interpolated array are all relative to the array center at $\frac{KN}{2}$. This procedure amounts to interpolation followed by decimation of the original data.

Angular Spectrum Estimation

This section outlines the minimum variance spectral estimation method used to derive the angular spectrum at each range bin. Consider an array of N sensors whose location and directional characteristics are known. Assume that there are multiple signal sources whose statistical characteristics are uncorrelated. A simple model for the received signal $y(t)$ at the output of each element can be expressed by:

$$\mathbf{y}(t) = \sum_{l=1}^L \mathbf{a}(\psi_l) x_l(t) + \mathbf{n}(t), \quad t = 1, \dots, M. \quad (8)$$

The vector $\mathbf{a}(\psi_l)$ is the spatial signature ($N \times 1$) that depends upon the angle of arrival ψ and x is a scalar associated with the l th signal source and incorporates the time variation of the signal. Assume there are L signal sources and M uncorrelated snapshots. $\mathbf{n}(t)$ is additive Gaussian noise. The signal received by the sensors is $\mathbf{y}(t)$ and it is an $N \times 1$ complex vector. As evident, the signal $\mathbf{y}(t)$ is a linear combination of the spatial signature and the additive noise. When the geometry of the array is linear with equally spaced sensors, the steering vector of the l th signal source is

$$\mathbf{a}(\psi_l) = [1 \quad e^{ja(\psi_l)} \quad e^{j2a(\psi_l)} \quad \dots \quad e^{j(N-1)a(\psi_l)}]^T, \quad \text{where}$$

$a(\psi_l) = kd \sin \psi_l$ represents spatial frequency, and d denotes sensor spacing. The source signal $x(t)$ and the noise $\mathbf{n}(t)$ are white Gaussian distributed with zero mean, statistically independent of the field signal(s). Consequently we have:

$$\begin{aligned} E[\mathbf{x}(t)] &= 0, \quad E[\mathbf{x}(t)\mathbf{x}'(t)] = \mathbf{I}, \\ E[\mathbf{n}(t)] &= 0, \quad E[\mathbf{n}(t)\mathbf{n}'(t)] = \sigma^2 \mathbf{I} \end{aligned} \quad (9)$$

where ' represents conjugate transposition. The stationarity assumption extends to both it's temporal and spatial properties. The spatial covariance matrix can be expressed as follows:

$$\begin{aligned} \mathbf{R} &= E[\mathbf{y}(t)\mathbf{y}^H(t)] = \mathbf{A}(\Psi)\mathbf{A}^H(\Psi) + \sigma^2 \mathbf{I} \\ &= \sum_{l=1}^L \mathbf{a}(\psi_l)\mathbf{a}^H(\psi_l) + \sigma^2 \mathbf{I} \end{aligned} \quad (10)$$

The rank of the covariance matrix for a single complex exponential field is one. When more signals are present, the individual covariance matrices will sum to increase the rank for each signal (e.g., three signals produces a covariance matrix of rank three).

Next, define the steering vector as a sequence of complex exponentials, which are chosen to cancel the plane-wave signal's propagation-related phase shift. This vector either steers the beam's assumed propagation direction to the wave's direction of propagation or focuses the beam in the case of a near-field source. The general form for the steering vector is:

$$\mathbf{e} = \begin{bmatrix} e^{-jk_m^0 \cdot \bar{x}_0} \\ \vdots \\ e^{-jk_m^0 \cdot \bar{x}_{N-1}} \end{bmatrix} \quad (11)$$

The notation \bar{k}_m^0 denotes the phase shift due to the wave's propagation at each sensor.

Adaptive Beamforming

The basic approach here is to solve a constrained, minimum mean-squared error, optimization problem. Many algorithms have been developed using this concept. The received signal $y(t)$ from antenna array is expressed as:

$$\mathbf{y}(t) = \mathbf{a}(\psi)x(t) + \mathbf{n}(t) \quad (12)$$

where \mathbf{a} is the spatial signature of the desired signal. Using the conventional beamforming approach described above, we may form a weight vector \mathbf{w} focus the array:

$$\hat{x}(t) = \mathbf{w}^H \mathbf{y}(t) \quad (13)$$

The objective is to maximize the output signal to interference-plus-noise ratio (SINR). For constrained optimization, instead of maximizing the output SINR directly, we minimize the mean-squared value of the weighted observations,

$$P_o = E \left[\left| \mathbf{w}^H \mathbf{y} \right|^2 \right] = \mathbf{w}^H \mathbf{R} \mathbf{w} \quad (14)$$

subject to a look-direction gain constraint.

Minimum Variance Beamforming

Consider an ideal, unit-amplitude signal, assumed to be propagating in the direction $\bar{\xi}$. The notation for this signal is $\mathbf{e}(\bar{\xi})$. The idea is to apply the weight vector \mathbf{w} to the sensor output. Any signal from the direction specified by \mathbf{e} should have unit gain. Noise and signal propagating from other direction should be suppressed. In this case, the constraint optimization problem is:

$$\min_{\mathbf{w}} E \left[\left| \mathbf{w}^H \mathbf{y} \right|^2 \right] \quad \text{subject to } \text{Re} \left[\mathbf{e}^H \mathbf{w} \right] = 1 \quad (15)$$

where the constraint $\text{Re} \left[\mathbf{e}^H \mathbf{w} \right] = 1$ ensures that the ideal signal has unit gain. The optimum weight vector that solves the optimization problem is given by [1]:

$$\mathbf{w}_o = \frac{\mathbf{R}^{-1} \mathbf{e}}{\mathbf{e}^H \mathbf{R}^{-1} \mathbf{e}} \quad (16)$$

It is evident that the optimum weight vector depends on two parameters: the correlation matrix \mathbf{R} and the direction of propagation $\bar{\xi}$. As different directions are scanned, the weights adapt to the signal and noise component of the observations. The beamformer output power is $P = \mathbf{w}_o^H \mathbf{R} \mathbf{w}_o$, in the assumed propagation

direction. The output power of the minimum variance beamformer is:

$$P^{MV}(\bar{\xi}) = \left[\mathbf{e}^H(\bar{\xi}) \mathbf{R}^{-1} \mathbf{e}(\bar{\xi}) \right]^{-1} \quad (17)$$

Covariance Matrix Estimation

To estimate \mathbf{R} from the available data, it must be derived from I.I.D. samples of \bar{x} , the observed data. The approach utilized for deriving multiple snapshots is perhaps the most important one for imaging since it can yield an array that does not sacrifice degrees of freedom as is required for sub-array averaging. This technique is based on the use of a set of orthogonal, closely spaced, sub-frequencies around each frequency m . By referring again to (3), (4) it is evident that another way to view the situation is that of a *moving* target within a single tone, continuous wave transmit field. With this Doppler shift in mind we can look at the work described earlier in a different way. If the transmitter is swept around each of M frequencies, in L steps of step size Dl/L , then the L sub-frequencies form an orthogonal set over a narrow frequency band. D is defined as the total bandwidth of the induced Doppler shift. Thus we have created a set of receive vectors \bar{x}_{ml} , that are uncorrelated signals to be used in (16). The total bandwidth utilized by the system is the same although it has been more finely divided. The resulting data cube is of size $N * M * L$. Ideally L would be equal to $2N$ since it can be shown that this value yields estimates of \mathbf{R} that are within 3dB of optimal. The resampling process is carried out for each frequency f_{ml} , as described above. After range compression is applied using the FFT (Fast Fourier Transform), the corresponding groups of \bar{x}_{ml} are used to build \mathbf{R} for that range bin, as shown by

$$\mathbf{R}_m = \frac{1}{L} \sum_{l=0}^{L-1} \bar{x}_{m+l-\frac{L}{2}} \bar{x}_{m+l-\frac{L}{2}}^* \quad (18)$$

Next is a brief description of forward-backward averaging, which is an effective way to improve a correlation matrix estimate. A ULA (uniform linear array) steering vector remains invariant up to a scaling if it's elements are reversed and complex conjugated. Let \mathbf{J} be an $N \times N$ exchange matrix whose components are zero except for the anti-diagonal. Then for the ULA it holds that $\mathbf{J} \bar{s}^*(\phi) = e^{-j(N-1)\rho} \bar{s}(\phi)$.

The backward array correlation matrix is therefore $\mathbf{R}_b = \mathbf{J}\mathbf{R}^*\mathbf{J}$. By averaging this matrix with the normal one we get the new correlation matrix

$$\mathbf{R}_{FB} = \frac{1}{2}(\mathbf{R} + \mathbf{J}\mathbf{R}^*\mathbf{J}). \quad (19)$$

By combining the methods outlined above we are able to estimate \mathbf{R} with a great deal of robustness. In general, \mathbf{R} will be full rank but may have a high condition number. We wish to obtain reasonable estimates in all normal imaging environments, so for this reason we include a user controllable amount of diagonal loading $\sigma^2\mathbf{I}$, added to \mathbf{R} to set the dynamic range of the image.

Computer Simulation Results

A computer simulation has been created to verify the proposed scheme for adaptive imaging. Figure 2 shows a image created by performing conventional beamforming on a 12-element array, using 800-1200 MHz bandwidth, and 40 frequency steps. The 8 targets are not discernible due to the antenna sidelobes. The 5 targets at 5 meters downrange are not separable. Figure 3 uses a 12-element array and 4 sub-frequencies but uses spatial resampling to achieve the best possible imaging. All targets are clearly discernible.

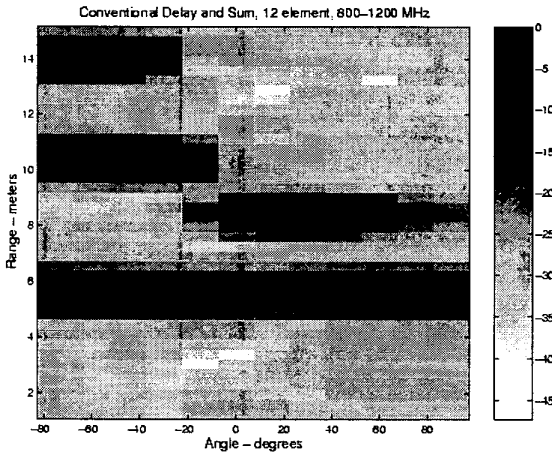


Figure 2. Conventional beamforming, using a 12-element array with 8 targets.

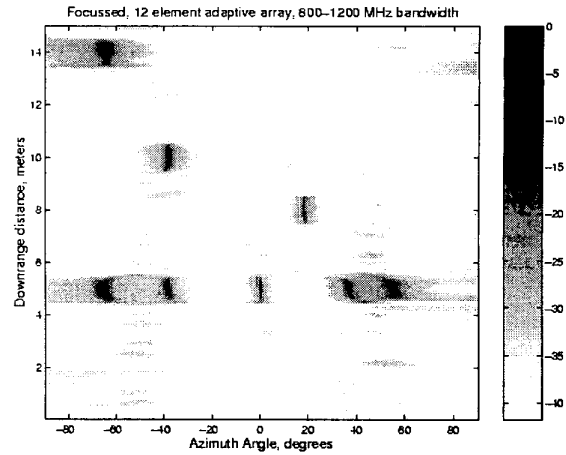


Figure 3. Resampled, Prefocused Adaptive array using 12-element array with 8 targets.

Experimental Results

The imaging system consists of a 4-element uniform linear array for receive, and a wide beamwidth horn antenna for the transmitter. The source is stepped from 800 MHz to 1200 MHz in 80 increments. The system center frequency is, $F_c = 1$ GHz or approximately 33cm wavelength and $\lambda_c = c_o/F_c$. Transmit power is 5dBm into the horn antenna. The receiver consists of 4 vertical half wave at λ_c , dipoles, spaced at half wave at λ_c intervals, followed by matched (equal group delay) receive channels, with 60dB gain, and each mixed to a 102.5 KHz IF frequency. The transmitted signal is tapped off at the antenna and mixed by the LO to 102.5 KHz to form the reference signal. The 5 signal channels are sampled at 10 KHz each, thus converting each signal to 2.5 KHz discrete time due to undersampling. This signal, being $1/4$ of the sample rate is then converted to complex baseband by mixing with digital quadrature oscillators, followed by low pass filtering. Finally, one set of 4 complex signals, representing S_{21} for each antenna is created by dividing each channel's baseband signal by the reference signal to derive the round trip phase and amplitude response at each antenna element for each frequency. The system is placed in an anechoic chamber for testing. Test objects consist of various metal cylinders, approximately 1-2 wavelength in size and placed from 3 to 8 meters away. It should be noted that our anechoic chamber is not highly effective at absorbing energy at 1GHz, so there is some clutter energy.

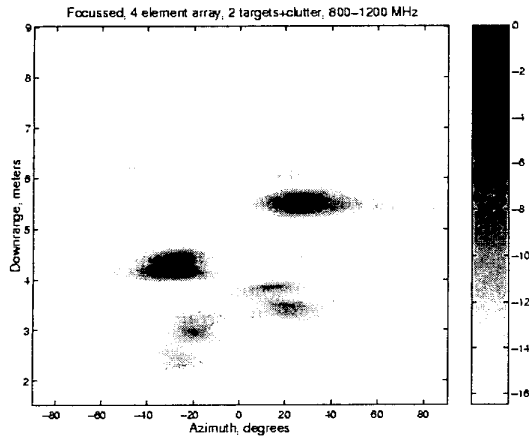


Figure 4. One target at 4.5m downrange and -30° crossrange, A larger cylindrical object is at 5.5m downrange and 25° crossrange.

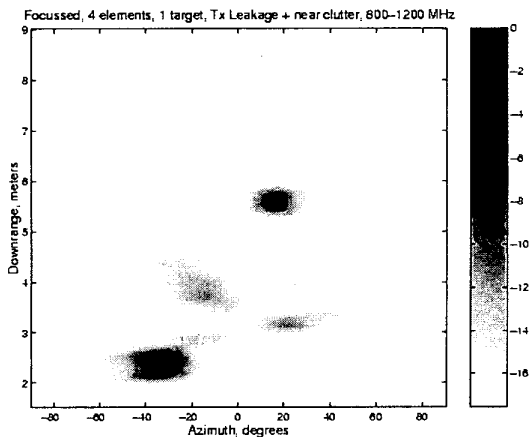


Figure 5. One small cylinder target at 5.5m downrange and $+20^\circ$ crossrange, transmitter is at 2.5m downrange and 30° crossrange. Near field clutter is seen between the transmitter and target.

The experimental array uses the same frequency and bandwidth parameters as the simulation except has 4 elements, utilizes forward-backward averaging, and 4 sub-frequencies. This array could benefit from using more sub-frequencies to improve the estimate of \mathbf{R} , but system constraints restricted the available data storage. Future hardware will allow more data storage as well as additional antenna elements. Diagonal loading is used to set the dynamic range of the image and stabilize the correlation matrix estimates. Figure 4 shows a image of 2 targets in the chamber. The available space is fairly small, consequently the target scenario is simple. Figure 5 shows

a higher level of near field clutter as well as some emitted signal from the transmitter horn.

Conclusion

This paper has outlined an approach for radar imaging using wideband array processing techniques. In particular the use of spatial resampling to convert signals to a narrowband model, and an induced Doppler shift for angular spectrum estimation are combined for imaging. Simulations were validated by an experimental 4-element, stepped CW system. Ongoing work will investigate larger arrays, performance issues, antenna element dispersion and calibration. This approach may be useful for automotive radar applications that utilize small patch antennas or foliage penetration systems that utilize low frequencies for imaging and area surveillance.

References

1. J.Capon, "High Resolution Frequency-Wavenumber Spectrum Analysis", Proceedings of the IEEE, 57:1408-1418, 1969
2. J.Krolik and D.Swingler, "Focused Wide-Band Array Processing by Spatial Resampling", IEEE Trans. Acoust., Speech, Signal Processing, vol. 38, No. 2, pp. 356-360, 1990.
3. R.A. Roberts and C.T. Mullis, "Digital Signal Processing", (Addison-Wesley), pp.447-448, 1987
4. S. Haykin, Editor, "Advances in Spectrum Analysis and Array Processing", (Prentice-Hall), VOL. I and II, 1991